ACS APPLIED MATERIALS & INTERFACES

Research Article

Cite This: ACS Appl. Mater. Interfaces 2019, 11, 16018−16026

www.acsami.org

Versatile and High-Throughput Polyelectrolyte Complex Membranes via Phase Inversion

Kazi Sadman,[†,§] David E. Delgado,[†,§] Yechan Won,[‡] Qifeng Wang,[†] Kimberly A. Gray,[‡] and Kenneth R. Shull*[,†]

[†]Department of Materials Science and Engineering and [‡]Department of Civil and Environmental Engineering, Northwestern University, Evanston, Illinois 60208, United States

Supporting Information

ABSTRACT: High-flux filtration membranes constructed through scalable and sustainable methods are desirable for energy-efficient separations. Often, these criteria are difficult to be reconciled with one another. Polymeric membranes can provide high flux but frequently involve organic solvents in processing steps. Solubility of many polymeric membranes in organic media also restricts their implementation in solvent filtration. In the present work, we report a simple and high-throughput aqueous processing approach for polyelectrolyte complex (PEC) membranes with controllable porosity and stability in various aqueous and organic environments. PECs are materials composed of oppositely charged polymer chains that can form solids in aqueous environments, yet which can be dissolved in very specific salt solutions capable of breaking the interpolymer ion pairs. By exploiting the salt-induced dissolution and subsequent reformation of the complex, nano- to microporous films are rapidly synthesized which resemble membranes obtained through conventional solvent-phase inversion techniques. PECs remain stable in organic solvents because of the low dielectric constant of the environment, which enhances electrostatic interactions, making them suitable for a wide range of water and solvent filtration applications. Here, we elucidate how the polymer-phase behavior can be manipulated to exercise morphological control, test membrane performance for water and solvent filtration, and quantify the mechanical stability of PECs in relevant conditions.

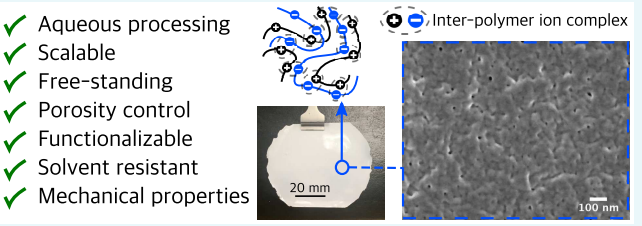

KEYWORDS: *High-flux filtration membranes, polyelectrolyte complex, coacervate, quartz crystal microbalance*

1. INTRODUCTION

Although the increasing demand for water, oil, and organic solvents is an intransigent reality of modern society, the energy requirement for processes used to obtain these commodities is not. Technological innovations can often improve process efficiency while delivering higher throughputs and better performances. A powerful example of this is the wide-scale adoption of reverse osmosis membranes for water desalination, which has nearly replaced thermal desalination. Yet, given the success of reverse osmosis membranes, the drive for enhanced scalability, sustainability, and cost/energy efficiency remains.[1]

The performance of a membrane is primarily a function of its porosity, thickness, and hydrophilicity. The degree to which it is possible to control these characteristics is contingent on the materials utilized and processes employed to form the membrane. Many polymeric membranes are synthesized using organic solvents, which provide control over thickness and porosity, but inherently render them unstable in organic environments. Several cross-linking strategies may be used to overcome this significant limitation, but they inevitably lead to more processing steps. It is highly desirable to develop a membrane where porosity and thickness can be controlled without compromising its integrity in application environments. It is also desirable to develop methods to produce scalable membranes while eliminating the use of organic solvents completely. Unfortunately, the adoption of sustainable methodologies and polymers into membrane technologies has been hindered by practical impediments such as incompatibility with existing at-scale processes and poor mechanical properties.

Polyelectrolyte complexes (PECs) offer several advantages to meet some of the challenges outlined above. These materials are composed of oppositely charged polyelectrolytes that can offer high water fluxes because of their charged chemistry and are processed from simple aqueous solutions that are environmentally benign. The component polyelectrolytes can be changed with minimal adjustments to process parameters, thus ascribing to these materials desirable robustness and tunability. Until now, PECs have been largely used for filtration membranes within the context of layer-by-layer (LbL) assemblies, where oppositely charged polyelectrolyte monolayers are built upon a substrate.[2−5] This approach is a powerful processing route because of its simplicity and minimal capital equipment requirement, thus making it an

Received: February 4, 2019
Accepted: April 8, 2019
Published: April 9, 2019

DOI: 10.1021/acsami.9b02115
ACS Appl. Mater. Interfaces 2019, 11, 16018−16026

exceptionally useful method when ultrathin films are required.[5−7] The LbL approach, however, is relatively time-consuming and therefore less amenable to scale up. It is also not appropriate in cases where thicker membranes, on the order of micrometers, are desired. Therefore, a significant advancement in the PEC membrane technology would be to reconcile the desirable properties of PECs with high-throughput membrane synthesis approaches, such as commercial-phase inversion techniques.[8,9]

When a polycation and a polyanion are mixed in a solution, they associate into a solid complex because of the large entropy gain from counterion release. This solid complex can be dissolved in appropriate salt solutions to form an associating polymer solution that can phase-separate into polymer-dilute and polymer-rich (coacervate) phases.[10,11] The coacervate phase is particularly unique as it can be considered a "molten" PEC, where salt and water are the analogues for temperature.[12] The coacervate phase is a liquid-like solution (10−35% polymer and 50−70% water depending on the salt concentration) that can be castor-extruded, similar to the traditional thermoplastic processing.[13,14] Although the temperature analogue for salt and PECs has recently gained currency, an alternate interpretation is that high ionic strength solutions are good solvents for the complex, whereas low ionic strength solutions are nonsolvents. Solvent quality in the traditional sense is predicated upon the relative polarity of the molecule of interest and solvent of choice. In the context of PECs, a good solvent is the one with sufficiently high ionic strength of a salt that can effectively break the interpolymer ion complexes that render the material solid-like. Because not all salts interact with complexes to the same extent, some salt solutions are better "solvents" than others. Generally, salts in which the cation and anion have a relatively high solvation free energy can break PEC ion pairs more efficiently than salts with lower solvation free energies.[11,15] In the present work, we utilize a PEC which only dissolves in KBr solutions, allowing the complex to be processed into films using this particular salt. Once formed, the PEC retains its mechanical integrity against all other common ions at moderate to high concentrations, making it suitable for a wide variety of filtration applications. The implications of salt identity with regard to stability and processability are further discussed in the manuscript.

Other important tenets of traditional membrane fabrication are porosity control and temporal process efficiency. In this respect, blade/bar cast polymer solutions that are subsequently rendered porous through phase inversion techniques, such as immersion precipitation, are a simple yet powerful method for achieving membranes or porous coatings.[8,16,17] In immersion precipitation, the polymer is dissolved in a good solvent, cast into a film, and then submerged in a second solvent that is miscible with the polymer solvent, but not the polymer. This process forces phase separation and typically leads to a porous microstructure capped by a dense skin layer.[18,19] The appearance of this skin layer is generally a surface-transport effect and can be rationalized using thermodynamic and kinetic arguments.[16] In many cases, the capping skin layer can provide selectivity while the porous substructure allows high flux and provides mechanical support.[16,20] This approach can be easily adapted for roll-to-roll processing at scale and is the preferred method for many commercially available membranes.[20] Moreover, porosity is controlled by modulating the composition of the initial polymer solution, and the whole process typically requires on the order of seconds to minutes to complete.[21,22] Constructing PEC membranes in this manner would overcome the limitations of LbL assembly, while eliminating the need for organic solvents in typical solvent-phase inversions, resulting in an overall greener process that remains scalable.

In the present work, we synthesize PEC membranes using a coacervate of anionic poly(styrene sulfonate) (PSS) and cationic poly(*N*-ethyl-4-vinylpyridinium) (QVP-C2). The PSS:QVP-C2 complex is dissolved in KBr solutions, which is one of the most effective salts for breaking interpolymer ion pairs, and where the ionic strength dictates the composition and viscosity of the coacervate phase. Here, the polymer−KBr−water phase behavior of the complex is utilized to form membranes with porosities ranging from nanometers to micrometers using a water−water phase inversion via immersion precipitation in a low ionic strength nonsolvent. We demonstrate that this traditional membrane fabrication methodology is well suited for processing PECs, where the coacervate phase replaces the polymer solution and ionic strength determines the solvent quality. We test the membrane performance in terms of rejection of polystyrene beads and polyethylene glycol (PEG) dispersed in water and demonstrate the versatility of PEC membranes by extending the feed solutions to organic solvents. Finally, we quantify the mechanical properties of the PSS:QVP-C2 complex and introduce strategies for further control over the stability, responsiveness, and functionality of these materials.

2. RESULTS AND DISCUSSION

The experimental results and their significance are discussed in the following sections. We first quantify the phase behavior of the model PEC of PSS and poly(*N*-ethyl-4-vinylpyridinium) (PSS:QVP-C2) as shown in Figure 1. PSS:QVP-C2 can be dissolved into a viscous polymer-rich coacervate phase at sufficiently high concentrations of KBr.[11] The associated phase behavior is then manipulated to control the porosity of the final membranes by judicious selection of the initial coacervate composition. Next, we quantify the mechanical stability of the solid complex in relevant salt solutions and in organic solvents. The flux of solvents through the membrane is discussed in comparison to pure water. Finally, we explore the versatility of PEC membranes using a simple surface modification using Nafion, which changes the flux of solvents based on their relative polarities.

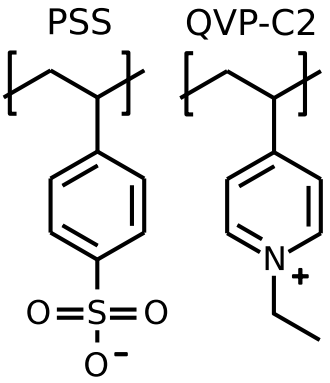

Figure 1. Structures of the polyelectrolytes used in this work.

2.1. PEC Phase Inversion. The concept of phase inversion has been extended to the PSS:QVP-C2 system, whose phase

DOI: 10.1021/acsami.9b02115
ACS Appl. Mater. Interfaces 2019, 11, 16018−16026

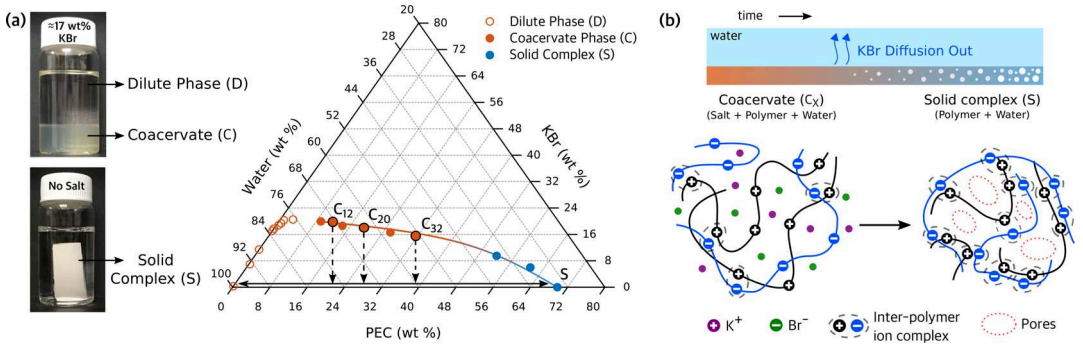

Figure 2. (a) Phase behavior of the PSS:QVP-C2 complex. In the absence of salt, the two polyelectrolytes neutralize each other into a solid complex, *S*. Increasing the salt concentration results in a liquid−liquid phase separation between a polymer-rich coacervate phase and a polymer-dilute phase.[10,11] The coacervate is a viscous polymer solution that can be cast into films of controllable thicknesses. (b) Schematic representation of the salt-mediated water−water phase inversion process. Immersion of a coacervate film into a low ionic strength solution drives salt out of the film, forcing a polymer/water phase separation that results in a porous microstructure. Here, composition of the coacervate can be modulated by changing the salt concentration which is inversely related to the total polymer concentration. The polymer concentration strongly affects the pore size distribution in immersion precipitations.[19] Coacervates of the composition C_X, where X is the polymer wt %, is used to control the degree of porosity of the final membrane (see Figure 3).

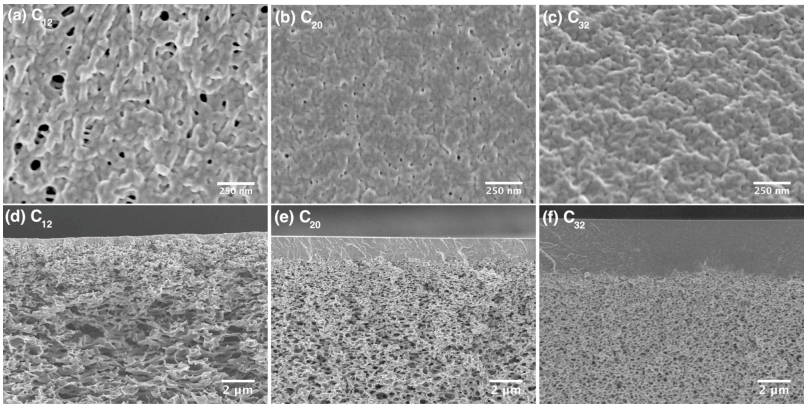

Figure 3. SEM images of the surface (a−c) and the corresponding cross sections (d−f) for membranes cast from initial coacervate compositions C_{12} (18.3 wt %), C_{20} (17.1 wt %), and C_{32} (15.1 wt %), where the subscripts correspond to the initial polymer fractions in the coacervate and the corresponding KBr fractions are reported in parentheses. Increasing the salt concentration increases the water content and reduces the polymer concentration in the coacervate, which results in a more porous surface and bulk microstructure. A dense "skin-layer" is observed at the membrane surface whose thickness diminishes as the membrane is made more porous. The porosity of the underlying substructure increases with increasing salt and water concentrations.

behavior is shown in Figure 2a. A solid complex of composition *S* (30% water, 70% polymer) is the stable composition in the absence of salt. Here, the intrinsic 30 wt % water content is a result of solvating the charges present within the complex. Clear, one-phase solutions are obtained for overall salt concentrations above ≈20 wt %. At salt concentrations below 20 wt %, the system separates into a phase with almost no polymer and polymer-rich coacervate phase with a polymer concentration that decreases with increasing salt concentrations. The addition of 15.1 wt % KBr results in a clear liquid-like coacervate with a polymer concentration of 32 wt %; hence, we refer to this coacervate solution as C_{32}. The addition of more salt further increases the water content of the coacervate, with a 17 wt % KBr giving a coacervate phase with a polymer concentration of 20 wt % (C_{20}) and a 18.3 wt % KBr giving a coacervate phase with a polymer concentration of 12 wt % (C_{12}). Solutions drawn from these coacervate phases can be cast into thin films using established blade or bar casting methods onto any desirable substrates. Upon immersing this film in pure water, an osmotic gradient is created, which forces the salt ions out of the film, driving the composition to point *S*. Because the polymer ion pairs are no longer screened by the salt ions, water becomes a poor solvent and phase separation occurs leaving the PEC into a porous structure with a capping layer, as can be seen in Figure 3d−f. This phase separation happens on the order of seconds to minutes and thus produces micrometer-thick films much faster than traditional LbL deposition.[7] A schematic representation of this process is depicted in Figure 2b, where the initial coacervate solution has a significant amount of salt water that plasticizes it. Contact with a low ionic strength solution extracts the salt, forcing the PEC to form a porous structure as it moves to its new equilibrium composition.

Porosity control can be achieved as increasing or decreasing the initial salt concentration, and thus the amount of polymer/water in the coacervate, which moves one left or right along the phase boundary. Aqueous immersion from these different starting points leads to varying final porosities, providing an easy tool to tailor morphology. By examining three different initial compositions (C_{12}, C_{20}, and C_{32}, subscript is the polymer wt %), we can carefully observe the morphological change in the final membrane. Figure 3a−c reveals that a range of surface

DOI: 10.1021/acsami.9b02115
ACS Appl. Mater. Interfaces 2019, 11, 16018−16026

porosities, from a completely dense layer to a layer with 10−100 nm pores, can be achieved. It is important to note that the thickness of the dense skin layer decreases as one increases the salt concentration as shown in Figure 3a−c. As the rate at which the microstructure forms is determined by the mobility of the polymer chains at the surface, the viscosity of the solution is critical, and in our case, this is a strong function of the salt concentration.[16,23] Thus, at lower salt concentrations (and higher viscosities due to higher polymer concentration), the mobility of the polymers are restricted, which is expected to lead to a slower microstructure evolution. Changes in surface porosity in response to the starting coacervate composition also correspond to differing porosities in the underlying substructure. Figure 3d−f shows that the substructure porosity also spans a wide range.

With different pore sizes and skin layer thicknesses, the membranes exhibited substantial differences in water flux as shown in Figure 4. Each increment in initial salt concentration

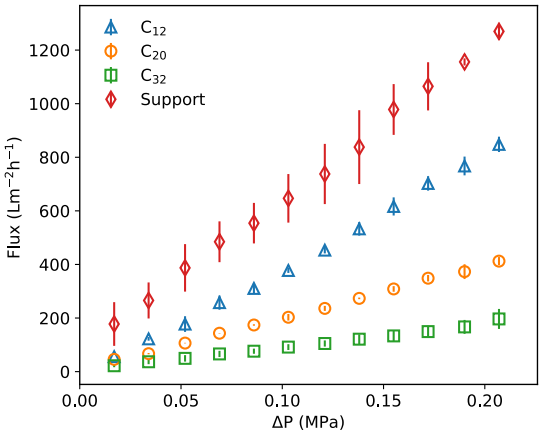

Figure 4. Flux measurements of membranes cast from different initial coacervate compositions. The membrane porosity decreases with increasing polymer concentrations in the starting coacervate solution, which manifests as a reduced water flux. The bare ceramic underlying support (+) is included for reference.

nearly doubled the water flux, confirming a variation in pore size and porosity in response to the initial salt concentrations. Furthermore, porosity control was quantified by looking at the rejection rate of polystyrene latex bead (PSL) and PEG of various sizes. Using eq 2, Table 1 shows that all three types of PECs achieved well above 95% rejection rate for PSL particles below 100 nm in size. They, however, showed relatively poor rejection for PEG with molecular weights below 1000 kDa. The rejection dropped further as the PEG molecular weight decreased or the pore size increased. Although the low PEG rejections for the C_{12} and C_{20} membranes can be rationalized from the pore sizes observed in the SEM images, the relatively high molecular cutoff for the C_{32} membrane, which appears to be quite dense as shown in Figure 3c and f, suggests that there may be defects. Because the phase inversion process is a highly nonequilibrium phenomenon, defect formation on the membrane surface is a possibility, and this may adversely affect the rejection capacity. Further investigations are necessary to corroborate these observations.

Figure 4 also displays the high fluxes at relatively low pressures that may be achieved from PEC membranes. This may be attributed to the diminishing skin layer thickness with increasing porosity, as well as to the overall water content of the membrane itself that arises from the highly charged nature of the material. On the basis of the result presented in Figure 4, the pure water permeance of C_{12}, C_{20}, and C_{32} membranes was calculated to be 95, 205, and 375 L m^{-2} h^{-1} bar^{-1} using eq 3, respectively. These values fall within the reported pure water permeance values of high-flux ceramic and polymer ultrafiltration membranes available in the market, which typically can range from ≈70 to 525 L m^{-2} h^{-1} bar^{-1}.[24−28] Using the flux measurements of Figure 4 in conjunction with Darcy's law (eq 1) for flow through a porous medium, it is possible to calculate a characteristic length scale for the PEC membranes from the water permeability, k_m[29]

$$k_m = \frac{Q\eta d}{A\Delta P} \tag{1}$$

Here, Q is the volumetric flow rate in m^3/s, A is the membrane area, d is the membrane thickness, η is the fluid viscosity, and ΔP is the pressure drop across the membrane. The characteristic length scale is given by $\sqrt{k_m}$, which we compute to be 5, 8, and 16 nm for C_{32}, C_{20}, and C_{12}, respectively. Here, we have calculated $\Delta P = \Delta P_{membrane+support} - \Delta P_{support}$ for a particular flux.

2.2. Stability of Membranes in Salts and Solvents. An important determinant for the point of use for a filtration membrane is its mechanical stability.[30] It is critical for membranes to have high flux and high tolerance to a wide range of feed solutions and operating conditions.[30−32] Some membrane applications may become limited by poor mechanical stability, limiting their use under the high pressures associated with nanofiltration, for example.[33,34] Because we have utilized concentrated KBr solutions to dissolve the solid-like PEC into a liquid-like coacervate solution, the relevant question is what is the stability of the complex in other salt solutions. It is probable that a water filtration membrane will encounter feed solutions composed of a variety of ions, and if the material integrity is compromised in the presence of salt ions, then the overall applicability of the material will be diminished.

Table 1. Rejection of Polystyrene Beads and PEG Macromolecules Using PEC Membranes[a]

	polystyrene bead rejection (%)					PEG MW (%)		
membrane	800 nm	600 nm	460 nm	300 nm	100 nm	1000 kDa	200 kDa	20 kDa
C_{32} (15.1%)	99.2 ± 0.1	99.7 ± 0.1	99.3 ± 0.2	97.5 ± 0.2	98.7 ± 2.5	87.1 ± 1.4	45.3 ± 2.8	11.9 ± 4.1
C_{20} (17.1%)	99.3 ± 0.1	98.9 ± 0.2	98.9 ± 0.2	99.8 ± 0.1	99.6 ± 0.2	70.7 ± 2.8	40.8 ± 0.5	2.24 ± 2.1
C_{12} (18.3%)	99.4 ± 0.1	99.6 ± 0.1	97.0 ± 1.7	97.6 ± 0.4	99.2 ± 0.9	32.3 ± 7.9	23.3 ± 3.3	0.9 ± 0.9

[a]Membranes were fabricated from the coacervates of composition C_X, where X is the polymer wt %. The corresponding KBr wt % of the coacervate is reported in parenthesis. Membranes made from lower KBr concentrations possessed a larger polymer fraction, which resulted in a less porous structure that showed better rejection of PEG. Errors were reported as the standard deviation of three measurements.

DOI: 10.1021/acsami.9b02115
ACS Appl. Mater. Interfaces 2019, 11, 16018−16026

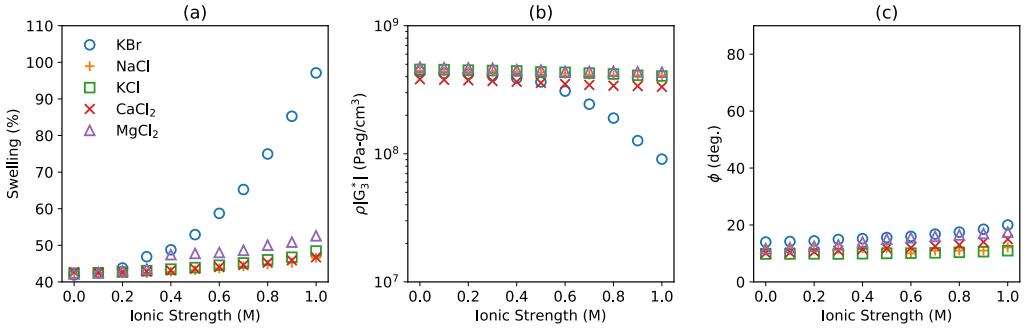

Figure 5. (a) Swelling %, (b) density-shear modulus product, and (c) viscoelastic phase angle at 15 MHz of PSS:QVP-C2 in response to increasing ionic strengths of different salt identities. KBr is the only salt that can effectively swell and dissolve this complex by breaking ion pairs between PSS and QVP-C2, while other salt ions do not significantly affect the mechanical integrity of the complex, and therefore also do not effectively dissolve the complex. This essentially allows PSS:QVP-C2 membranes to be processed from KBr solutions, while maintaining stability in a variety of commonly encountered salts at ambient to high concentrations. A ≈43% increase in thickness relative to that of a dry film is observed for the complex-immersed pure water, which is attributed to charge hydration. Viscoelastic properties and the swelling ratio were measured at 15 MHz using the QCM as described previously.[11,35] PEC films (≈1 μm) were spun-cast from an equilibrated coacervate of PSS:QVP-C2 directly on to the quartz crystal for measurements.[11,14] For reference, polymer glasses have a shear modulus of ≈2 × 10^9 Pa and a $\phi \approx 1°$ at this frequency, and $G^* = G' + iG''$ and $\phi = \arctan(G''/G')$ as usual.

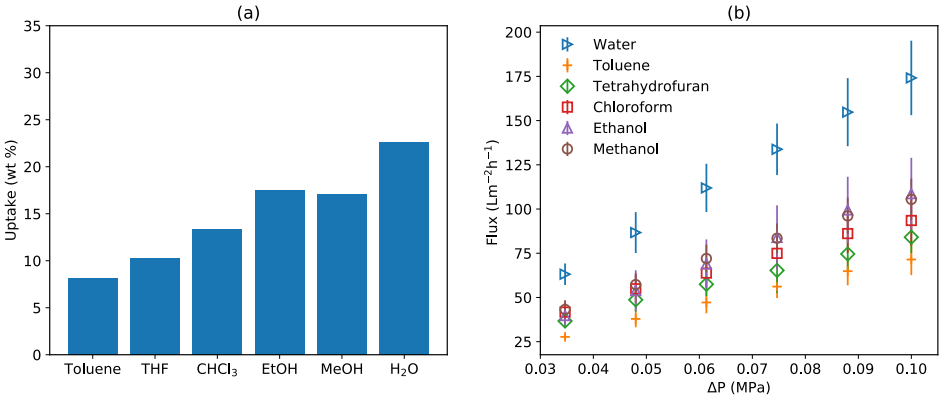

Figure 6. (a) Solvent uptake of the PSS:QVP-C2 complex with respect to the film in air, which already contains ≈13% water of solvation from ambient humidity. Nonpolar solvents interact weakly with the charged complex, whereas polar solvents interact more strongly.[41] (b) Solvent flux through the C_{20} membrane scales with the ability of the solvent molecule to interact with the complex. The static water contact angle of this PSS:QVP-C2 membrane was measured to be 32 ± 5°. This inherent hydrophilicity of the material results in a high water flux.

To investigate the robustness of these membranes in different salt solutions, the PEC materials were characterized using the quartz crystal microbalance (QCM). This technique is advantageous because it allows mechanical characterization while simultaneously measuring the swelling ratio of homogeneous and pore-free thin films with a high precision.[11,35,36] The swelling ratio is directly related to the water content of the PEC films, and the QCM reports the density-shear modulus product at 15 MHz ($\rho|G_3^*|$) and the associated viscoelastic phase angle (ϕ) of the material deposited on the crystal. For further information on this technique and its capability for in situ mechanical measurements, the reader is directed to previous literature studies.[11,35,36] Figure 5 shows that the PSS:QVP-C2 complex remains stable in all common salt solutions, with little swelling at up to 1.0 M ionic strength. Correspondingly, $\rho|G_3^*|$ remains nearly constant in this salt concentration regime, and ϕ remains low, indicating that the materials are primarily elastic. KBr was the only ion combination to effectively swell the complex and diminish $\rho|G_3^*|$ because both potassium and bromine being poorly solvated ions.[11,13,14] This selective salt responsiveness is extremely beneficial as it allows the PEC to be processed like a traditional polymer with concentrated KBr solutions while preserving resistance to common ions. This stability of the complex in salts other than KBr also demonstrates that most salts are not suitable for the fabrication of PEC membranes as they would either require a very high concentration or be completely incapable of swelling the PEC and forming the coacervate phase. Nevertheless, some polyanion/polycation combinations may be processed using concentrated NaCl solutions.[37] The salt resistance of the PEC can also be systematically tailored by controlling the hydrophobicity[11] or the ion-pairing affinity[36] of the component polyelectrolytes, while retaining orthogonal control over the porosity through the phase behavior. An informative comparison here is of PSS:QVP-C2 to seawater, which has a ionic strength between 0.5 and 0.6 M and is primarily enriched in sodium, calcium, magnesium, and chlorine.[38] Therefore, based on Figure 5, PSS:QVP-C2 membranes are expected to be stable in seawater, where the bromine concentration is low. Figure 5 also shows that PSS:QVP-C2 swells about 43% relative to the completely dry film when immersed in pure water. This is the inherent water content of the material, which primarily results from solvation of the charged monomer units. This allows the complex to conduct water efficiently and makes them naturally hydrophilic, which ultimately results in higher

DOI: 10.1021/acsami.9b02115
ACS Appl. Mater. Interfaces 2019, 11, 16018−16026

water fluxes at lower porosities. Although in the present work we do not explore the pH stability of the complex, these materials are expected to operate in pH ranges of 2−13, as both PSS (pK_a = 1) and QVP-C2 are strong polyelectrolytes.[39]

A further advantage of the PEC membranes is their stability in organic solvents that can limit performance in traditional polymeric membrane materials.[9,40,41] Without additional processing or modification, the PSS:QVP-C2 films were subjected to a variety of common solvents on the QCM and found to have lower solvent uptake compared to water as depicted in Figure 6a. The solvent flux also scales with the relative interaction of the solvent molecules to the PEC material, as shown in Figure 6b. This stability is due to the low dielectric constants of these solvents that enhances electrostatic interactions between the oppositely charged chains. In traditional polyolefins, low dielectric solvents are good solvents, a limitation that can be overcome by cross-linking strategies. This inevitably leads to more chemical modification and processing steps. In the present case, the electroneutrality condition and strong electrostatic correlations in low dielectric environments act as natural cross-links for the material. Solvent flux is then affected by the dielectric constant, polarity, and membrane surface porosity of the solvent. Solvents with a high dielectric constant, such as water, swell the membrane and interact favorably with the membrane surface, as observed from the low water contact angles of ≈30° for the PEC.[42] Flux tests were performed as shown in Figure 6b to investigate the suitability of PEC membranes for organic solvent filtration. Solvents such as toluene, tetrahydrofuran, and chloroform with dielectric constants of 2.38, 7.58, and 4.81, respectively, had lower flux rates (and lower swelling) compared to ethanol, methanol, and water with dielectric constants of 24.5, 32.7, and 80, respectively. In addition, Fares et al. have demonstrated that solvents with a molecular size less that 50 Å^3 seems to be a requisite for effectively swelling PEC complexes and thus could influence flux.[41] Overall, the capacity of these PEC membranes to treat both aqueous and organic solutions without complex or expensive chemical modification speaks to the versatility of these materials while being a potential greener alternative to current technologies.

2.3. Tuning Hydrophobicity through Surface Modification. Beyond development of new membrane materials, surface functionalization allows membranes to be further tailored for filtration needs.[43] Although there has been a wide suite of techniques developed, such as surface grafting and plasma treatment, they often require additional processing steps, chemical modification, or instrumentation.[44−46] It is attractive to utilize simpler methods such as adsorption, which can be inexpensive and more amenable to large-scale production. One modification strategy is to modify surface hydrophobicity. This property plays a key role in determining membrane effectiveness in many applications, including those where the flux of nonpolar molecules through the membrane needs to be controlled. In order to produce hydrophobic membranes, the PEC membranes here were immersed in a dilute Nafion solution, allowing the sulfonic acid group of Nafion to bind with the charged PEC membrane.[42] The static contact angle increased from ≈30° to ≈100° upon Nafion functionalization. These Nafion-functionalized membranes were subjected to both water and solvent flux tests. Figure 7 shows that the flux of polar solvents decreased in general after Nafion functionalization, with water having the most reduction in flux (by ≈80%) relative to the native performance of the membrane as shown in Figure 6b. Correspondingly, the flux of nonpolar solvents such as toluene and tetrahydrofuran increased by 42 and 33%, respectively. This result indicates a successful hydrophobic modification of the PEC membrane via the Nafion treatment. Indeed, this simple tuning of membrane hydrophobicity demonstrates the potential for simple surface tuning to fit specific applications.

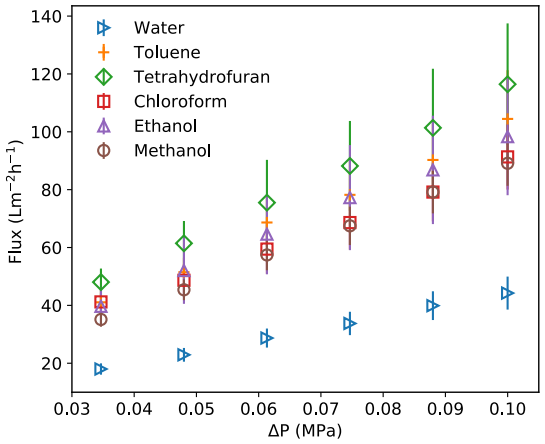

Figure 7. Solvent flux through a Nafion-functionalized C_{20} PSS:QVP-C2 membrane. The static water contact angle of the Nafion-functionalized membrane was measured to be 98 ± 4°. This resulted in a significantly diminished water flux and a much enhanced solvent flux relative to the unmodified membrane (Figure 6b).

3. CONCLUSIONS

In this work, we utilized a salt-induced phase inversion process from aqueous solution to rapidly fabricate robust membranes of PECs with controllable porosities for filtration applications. The advantages of PEC membranes, such as high water flux and inherent stability in solvents, can now potentially be realized at an industrial scale while utilizing a solvent-free process. A ternary phase diagram was constructed to guide intuition about changes in the PEC morphology induced by different compositions. By changing the composition of the initial complex coacervate through salt concentration, one moves along the phase boundary, and upon aqueous immersion obtains different pore sizes. These different microstructures were characterized with scanning electron microscopy (SEM) and by filtration experiments with well-defined PSL beads and PEG solutions. It was found that the rejection of these model impurities improved as the PEC membranes were made from solutions with lower salt concentrations. This trend was attributed to the formation of a thicker skin layer with smaller overall pore sizes from polymer solutions with a high initial polymer concentrations. The QCM was used to quantify the swelling and mechanical behavior of PEC thin films, and it was shown that the films were stable in all common salts, except KBr which can effectively dissolve the complex. Thus, these membranes are processable from KBr solutions while remaining stable in the presence of more common ions encountered in filtration contexts. Moreover, a variety of solvents minimally swelled these PEC membranes. Therefore, these complexes are applicable to a wide range of filtration applications without additional chemical modifications or processing steps. Finally, PEC membranes were immersed in a Nafion solution to easily change the hydrophobicity of the material. A reduction in

DOI: 10.1021/acsami.9b02115
ACS Appl. Mater. Interfaces 2019, 11, 16018−16026

water flux and a corresponding increase in toluene/tetrahydrofuran flux demonstrated the simplicity with which the functionality of these membranes may be tailored.

4. EXPERIMENTAL SECTION

4.1. Materials. PSS sodium salt MW 200 K g mol^{-1}) was purchased from Sigma-Aldrich. Poly(4-vinylpyridine) (P4VP, MW 50K g mol^{-1}) was purchased from Scientific Polymers. 1-Bromoethane, Nafion solution, NaCl, KCl, $MgCl_2$, $CaCl_2$, and KBr were also purchased from Sigma-Aldrich. Deionized water (conductivity ≈ 5 μS/cm) was used for preparing all solutions except while forming coacervates where 18.2 M Ω·cm MilliQ water was used.

4.2. Quaternization of P4VP. Ethyl-quaternized P4VP (QVP-C2) was synthesized by dissolving 10 wt % P4VP in dimethyl sulfoxide (DMSO) before adding 30% molar excess of bromoethane. The solution was then well stirred for 24 h at 40 °C.

4.3. Stoichiometric PECs. PECs were synthesized as reported previously.[11] Briefly, once the quaternization reaction was completed (in DMSO), the moles of QVP repeat units were calculated, and the equivalent amount of PSS was dissolved in the equivalent volume of water separately. The two solutions were then simultaneously added to a third beaker of water under stirring. The PECs again precipitated out as a white solid that was washed with deionized water until the solution conductivity fell to about 50 μS/cm. As pyridines have poor thermal stability, these precipitates were dried at 60 °C in the presence of drierite for 12 h to obtain the dry PEC.

4.4. Coacervates. Coacervates were formed from the dry PECs by dissolving them in solutions of KBr. In all cases, 1.50 g of dry PEC was dissolved in 10 g of MilliQ water (18.2 M varOmega cm) and 2.95, 3.45, or 3.70 g of KBr. Once the PECs dissolved, an additional 5 g of water was added while keeping the solution well stirred. This resulted in salt weight fractions of about 15.1 and 17.1, and 18.3% in the coacervate phase. Once the coacervate phase began to form, the solution was annealed at 60 °C for 30 min. The solutions were then allowed to equilibrate between 1 day and 1 month, depending on the sample. Coacervates formed at lower salt concentrations required longer equilibration times.

4.5. Membrane Fabrication. The viscous coacervate was cast onto a 2 × 2 in. polished aluminum 6061 plate using an Accugate Fluid Spreader (Wallingfor, VT). A ≈100 μm gap height was used for all films. The film was then immersed into a bath of deionized water to extract the salt from the film and thus causing pore formation. After immersion in the deionized water for 30 min, the porous film was then transferred into a bath of pH 13 water, which partially dissolved the underlying substrate and released a free-standing membrane. Each membrane was left immersed in pure water overnight to extract residual salt from the complex before further measurements. Salt diffusion out of PEC thin films generally occur on the order of hours.[47]

4.6. Membrane Performance Tests. A cross-flow filtration system (EMD Millipore MinitanTM system) equipped with a variable speed peristaltic pump and a pulse dampener was used to apply pressure difference across the membrane. The free-standing membrane supported by a zirconium oxide-based porous ceramic membrane (1.4 μm; Sterlitech) was then tested for performance in terms of its ability to reject PSL beads (particle size 100−800 nm; Sigma-Aldrich) and PEG (MW 20k to 1000k; Sigma Aldrich) at a fixed transmembrane pressure of 10 psi. PEG feed solutions were made at 0.06 mg/mL. UV−vis spectroscopy (Shimadzu UV-2450 UV−vis spectrophotometer) and DOC analysis (Teledyne/Tekmar Dohrmann Series Apollo 9000 Total Organic Carbon Analyzer) were used to determine the PSL and PEG rejection, respectively. The following equation was used to calculate the percent rejection of the target PSL and PEG:[48]

$$R = \left(1 - \frac{C_p}{C_f}\right) \times 100 \tag{2}$$

where R is the percent rejection, C_p is the permeate concentration, and C_f is the feed concentration. The membrane flux under variable transmembrane pressure was also measured. The membrane was subjected to a transmembrane pressure up to 30 psi with an increment of 2.5 psi with ultrapurified deionized water. The permeate mass and time were recorded to calculate the membrane flux rate, J, at a given transmembrane pressure using the following equation[48]

$$J = \frac{V}{(A_m \times t)} = \frac{M}{(A_m \times t \times \rho)} \tag{3}$$

where V, M, ρ, t, and A_m are the permeate volume, mass, density, filtration time, and filtration area, respectively. As for the solvent flux measurements, Welch self-cleaning dry vacuum systemTM (model 2027; variable pressure control from 2 to 760 Torr) equipped with a glass vacuum filtration assembly was used, for the cross-flow filtration system had poor chemical resistance against the solvents used.

4.7. PEC Mechanical Test. Swelling and high-frequency rheological characterizations (15 MHz frequency) of PECs were conducted using a QCM. A custom QCM holder (AWSensors, Valencia, Spain) was used in conjunction with a N2PK impedance analyzer (Thornhill, Canada) for swelling and viscoelastic measurements of spin-coated PEC films. PEC films (1.5 μm) were directly spin-coated onto 1″ quartz crystals with Au electrodes (Inficon, East Syracuse, NY) from the polymer-rich coacervate phase. The tests provided the swelling response and the corresponding shear modulus as a function of the solution ionic strength. More detailed description of the QCM usage for mechanical characterization was reported previously.[11,35,36] The open source QCM-D data analysis software was used to obtain mechanical properties.[49] The PEC film was then dried over hot drierite to remove all water, and the dry areal mass, $(d\rho)_{dry}$, was recorded using the QCM. Here, d is the film thickness and ρ is the density. The swelling ratio after immersion salt solutions was then computed using eq 1.

$$\text{Swelling \%} = \frac{\text{weight}_{\text{water+salt}}}{\text{weight}_{\text{polymer}}} \times 100 = \frac{(d\rho)_{\text{solution}} - (d\rho)_{\text{dry}}}{(d\rho)_{\text{dry}}} \times 100 \tag{4}$$

4.8. Phase Behavior. The phase behavior of PSS:QVP-C2 was measured using thermogravimetric and conductivity experiments. As PECs are a three-component system of water, salt, and polymer, only the fraction of two components need to be known to calculate the phase diagram. The water content of the solid complexes, coacervates, and the dilute phases was determined by drying them in an oven at 70 °C, and the salt content was measured using a conductivity meter calibrated against a known KBr calibration curve (Figure S3). A known mass of the solid complex, coacervate, or the dilute phase (typically ≈0.25 g) was added to 20 g of water. The sample was then allowed to equilibrate for 24 h to extract all the KBr and then the conductivity of the solution was measured. The calibration curve was then used to determine the mass fraction of KBr in the starting sample. The polymer weight fraction was then calculated by noting that the percentages must add to 100.

4.9. Scanning Electron Microscopy. PEC films were fabricated as previously described onto a silicon substrate but not floated off. The film was then immersed in a bath of liquid nitrogen, fractured, and placed on a 90° SEM stub. Osmium tetroxide was deposited on both top-down and cross-sectional samples to prevent beam damage. Images were taken using a Hitachi SU8030 cold source field emission SEM (Tokyo, Japan).

■ ASSOCIATED CONTENT

Supporting Information

The Supporting Information is available free of charge on the ACS Publications website at DOI: 10.1021/acsami.9b02115.

DOI: 10.1021/acsami.9b02115
ACS Appl. Mater. Interfaces 2019, 11, 16018−16026

UV−vis curves of different PSL bead solutions, PSL bead permeate, and feed solutions, and KBr conductivity calibration curve (PDF)

AUTHOR INFORMATION

Corresponding Author

*E-mail: k-shull@northwestern.edu.

ORCID

Kazi Sadman: 0000-0003-2872-752X

Kenneth R. Shull: 0000-0002-8027-900X

Author Contributions

§K.S. and D.E.D. contributed equally to this work.

Notes

The authors declare no competing financial interest.

ACKNOWLEDGMENTS

The authors thank Thomas Wu and Gavrielle Welbel for their help on performing some of the experiments. This work was supported by the National Science Foundation (NSF DMR-1710491) and made use of the MatCI Facility which receives support from the MRSEC Program (NSF DMR-1121262) of the Materials Research Center at Northwestern University. The authors also utilized the EPIC facility of Northwestern University's NUANCE Center, which has received support from the Soft and Hybrid Nanotechnology Experimental (SHyNE) Resource (NSF ECCS-1542205), the MRSEC program (NSF DMR-1720139) at the Materials Research Center, the International Institute for Nanotechnology (IIN), the Keck Foundation, and the State of Illinois, through the IIN.

REFERENCES

(1) Sholl, D. S.; Lively, R. P. Seven Chemical Separations to Change the World. *Nature* **2016**, *532*, 435.

(2) Stanton, B. W.; Harris, J. J.; Miller, M. D.; Bruening, M. L. Ultrathin, Multilayered Polyelectrolyte Films as Nanofiltration Membranes. *Langmuir* **2003**, *19*, 7038−7042.

(3) Yang, S. Y.; Ryu, I.; Kim, H. Y.; Kim, J. K.; Jang, S. K.; Russell, T. P. Nanoporous Membranes with Ultrahigh Selectivity and Flux for the Filtration of Viruses. *Adv. Mater.* **2006**, *18*, 709−712.

(4) Li, X.; De Feyter, S.; Chen, D.; Aldea, S.; Vandezande, P.; Du Prez, F.; Vankelecom, I. F. J. Solvent-Resistant Nanofiltration Membranes Based on Multilayered Polyelectrolyte Complexes. *Chem. Mater.* **2008**, *20*, 3876−3883.

(5) Cheng, W.; Liu, C.; Tong, T.; Epsztein, R.; Sun, M.; Verduzco, R.; Ma, J.; Elimelech, M. Selective Removal of Divalent Cations by Polyelectrolyte Multilayer Nanofiltration Membrane: Role of Polyelectrolyte Charge, Ion Size, and Ionic Strength. *J. Membr. Sci.* **2018**, *559*, 98−106.

(6) Shan, W.; Bacchin, P.; Aimar, P.; Bruening, M. L.; Tarabara, V. V. Polyelectrolyte Multilayer Films as Backflushable Nanofiltration Membranes with Tunable Hydrophilicity and Surface Charge. *J. Membr. Sci.* **2010**, *349*, 268−278.

(7) Hammond, P. T. Engineering Materials Layer-by-Layer: Challenges and Opportunities in Multilayer Assembly. *AIChE J.* **2011**, *57*, 2928−2940.

(8) Paul, M.; Jons, S. D. Chemistry and Fabrication of Polymeric Nanofiltration Membranes: A Review. *Polymer* **2016**, *103*, 417−456.

(9) Marchetti, P.; Jimenez Solomon, M. F.; Szekely, G.; Livingston, A. G. Molecular Separation with Organic Solvent Nanofiltration: A Critical Review. *Chem. Rev.* **2014**, *114*, 10735−10806.

(10) Liu, Y.; Momani, B.; Winter, H. H.; Perry, S. L. Rheological Characterization of Liquid-to-Solid Transitions in Bulk Polyelectrolyte Complexes. *Soft Matter* **2017**, *13*, 7332−7340.

(11) Sadman, K.; Wang, Q.; Chen, Y.; Keshavarz, B.; Jiang, Z.; Shull, K. R. Influence of Hydrophobicity on Polyelectrolyte Complexation. *Macromolecules* **2017**, *50*, 9417−9426.

(12) Spruijt, E.; Sprakel, J.; Lemmers, M.; Stuart, M. A. C.; van der Gucht, J. Relaxation Dynamics at Different Time Scales in Electrostatic Complexes: Time-Salt Superposition. *Phys. Rev. Lett.* **2010**, *105*, 208301.

(13) Shamoun, R. F.; Reisch, A.; Schlenoff, J. B. Extruded Saloplastic Polyelectrolyte Complexes. *Adv. Funct. Mater.* **2012**, *22*, 1923−1931.

(14) Kelly, K. D.; Schlenoff, J. B. Spin-Coated Polyelectrolyte Coacervate Films. *ACS Appl. Mater. Interfaces* **2015**, *7*, 13980−13986.

(15) Marcus, Y. Effect of Ions on the Structure of Water: Structure Making and Breaking. *Chem. Rev.* **2009**, *109*, 1346−1370.

(16) Hołda, A. K.; Vankelecom, I. F. J. Understanding and Guiding the Phase Inversion Process for Synthesis of Solvent Resistant Nanofiltration Membranes. *J. Appl. Polym. Sci.* **2015**, *132*, 42130.

(17) Mandal, J.; Fu, Y.; Overvig, A. C.; Jia, M.; Sun, K.; Shi, N. N.; Zhou, H.; Xiao, X.; Yu, N.; Yang, Y. Hierarchically Porous Polymer Coatings for Highly Efficient Passive Daytime Radiative Cooling. *Science* **2018**, *362*, 315−319.

(18) Smolders, C. A.; Reuvers, A. J.; Boom, R. M.; Wienk, I. M. Microstructures in Phase-Inversion Membranes. Part 1. Formation of Macrovoids. *J. Membr. Sci.* **1992**, *73*, 259−275.

(19) van de Witte, P.; Dijkstra, P. J.; van den Berg, J. W. A.; Feijen, J. Phase Separation Processes in Polymer Solutions in Relation to Membrane Formation. *J. Membr. Sci.* **1996**, *117*, 1−31.

(20) Warsinger, D. M.; et al. A Review of Polymeric Membranes and Processes for Potable Water Reuse. *Prog. Polym. Sci.* **2018**, *81*, 209−237.

(21) Lee, K.-W.; Seo, B.-K.; Nam, S.-T.; Han, M.-J. Trade-off between Thermodynamic Enhancement and Kinetic Hindrance during Phase Inversion in the Preparation of Polysulfone Membranes. *Desalination* **2003**, *159*, 289−296.

(22) Han, M.-J.; Bhattacharyya, D. Changes in Morphology and Transport Characteristics of Polysulfone Membranes Prepared by Different Demixing Conditions. *J. Membr. Sci.* **1995**, *98*, 191−200.

(23) Mousavi, S. M.; Zadhoush, A. Investigation of the Relation between Viscoelastic Properties of Polysulfone Solutions, Phase Inversion Process and Membrane Morphology: The Effect of Solvent Power. *J. Membr. Sci.* **2017**, *532*, 47−57.

(24) Huisman, I. H.; Dutré, B.; Persson, K. M.; Trägårdh, G. Water Permeability in Ultrafiltration and Microfiltration: Viscous and Electroviscous Effects. *Desalination* **1997**, *113*, 95−103.

(25) Shukla, R.; Balakrishnan, M.; Agarwal, G. P. Bovine Serum Albumin-Hemoglobin Fractionation: Significance of Ultrafiltration System and Feed Solution Characteristics. *Bioseparation* **2000**, *9*, 7−19.

(26) Mehta, A.; Zydney, A. L. Permeability and Selectivity Analysis for Ultrafiltration Membranes. *J. Membr. Sci.* **2005**, *249*, 245−249.

(27) Antón, E.; Álvarez, J. R.; Palacio, L.; Prádanos, P.; Hernández, A.; Pihlajamäki, A.; Luque, S. Ageing of Polyethersulfone Ultrafiltration Membranes under Long-Term Exposures to Alkaline and Acidic Cleaning Solutions. *Chem. Eng. Sci.* **2015**, *134*, 178−195.

(28) Wu, H.; Liu, Y.; Mao, L.; Jiang, C.; Ang, J.; Lu, X. Doping Polysulfone Ultrafiltration Membrane with TiO2-PDA Nanohybrid for Simultaneous Self-Cleaning and Self-Protection. *J. Membr. Sci.* **2017**, *532*, 20−29.

(29) Chen, S. H.; Willis, C.; Shull, K. R. Water Transport and Mechanical Response of Block Copolymer Ion-Exchange Membranes for Water Purification. *J. Membr. Sci.* **2017**, *544*, 388−396.

(30) Wang, K.; Abdalla, A. A.; Khaleel, M. A.; Hilal, N.; Khraisheh, M. K. Mechanical Properties of Water Desalination and Wastewater Treatment Membranes. *Desalination* **2017**, *401*, 190−205.

(31) Zondervan, E.; Zwijnenburg, A.; Roffel, B. Statistical Analysis of Data from Accelerated Ageing Tests of PES UF Membranes. *J. Membr. Sci.* **2007**, *300*, 111−116.

(32) Tashvigh, A. A.; Chung, T.-S. Facile Fabrication of Solvent Resistant Thin Film Composite Membranes by Interfacial Cross-

DOI: 10.1021/acsami.9b02115
ACS Appl. Mater. Interfaces 2019, 11, 16018−16026

linking Reaction between Polyethylenimine and Dibromo-p-Xylene on Polybenzimidazole Substrates. *J. Membr. Sci.* **2018**, *560*, 115−124.
(33) Geise, G. M.; Lee, H.-S.; Miller, D. J.; Freeman, B. D.; McGrath, J. E.; Paul, D. R. Water Purification by Membranes: The Role of Polymer Science. *J. Polym. Sci., Part B: Polym. Phys.* **2010**, *48*, 1685−1718.
(34) Yeo, J.; Kim, S. Y.; Kim, S.; Ryu, D. Y.; Kim, T.-H.; Park, M. J. Mechanically and Structurally Robust Sulfonated Block Copolymer Membranes for Water Purification Applications. *Nanotechnology* **2012**, *23*, 245703.
(35) Sadman, K.; Wiener, C. G.; Weiss, R. A.; White, C. C.; Shull, K. R.; Vogt, B. D. Quantitative Rheometry of Thin Soft Materials Using the Quartz Crystal Microbalance with Dissipation. *Anal. Chem.* **2018**, *90*, 4079−4088.
(36) Sadman, K.; Wang, Q.; Shull, K. R. Guanidinium Can Break and Form Strongly Associating Ion Complexes. *ACS Macro Lett.* **2019**, *8*, 117−122.
(37) Ali, S.; Prabhu, V. Relaxation Behavior by Time-Salt and Time-Temperature Superpositions of Polyelectrolyte Complexes from Coacervate to Precipitate. *Gels* **2018**, *4*, 11.
(38) Huber, C.; Klimant, I.; Krause, C.; Werner, T.; Mayr, T.; Wolfbeis, O. S. Optical Sensor for Seawater Salinity. *Fresenius. J. Anal. Chem.* **2000**, *368*, 196−202.
(39) Lewis, S. R.; Datta, S.; Gui, M.; Coker, E. L.; Huggins, F. E.; Daunert, S.; Bachas, L.; Bhattacharyya, D. Reactive Nanostructured Membranes for Water Purification. *Proc. Natl. Acad. Sci. U.S.A.* **2011**, *108*, 8577−8582.
(40) Vanherck, K.; Koeckelberghs, G.; Vankelecom, I. F. J. Crosslinking Polyimides for Membrane Applications: A Review. *Prog. Polym. Sci.* **2013**, *38*, 874−896.
(41) Fares, H. M.; Wang, Q.; Yang, M.; Schlenoff, J. B. Swelling and Inflation in Polyelectrolyte Complexes. *Macromolecules* **2019**, *52*, 610−619.
(42) Ghoussoub, Y. E.; Schlenoff, J. B. Janus Nanofilms. *Langmuir* **2016**, *32*, 3623−3629.
(43) Kochkodan, V.; Hilal, N. A Comprehensive Review on Surface Modified Polymer Membranes for Biofouling Mitigation. *Desalination* **2015**, *356*, 187−207.
(44) Miller, D. J.; Dreyer, D. R.; Bielawski, C. W.; Paul, D. R.; Freeman, B. D. Surface Modification of Water Purification Membranes. *Angew. Chem., Int. Ed.* **2017**, *56*, 4662−4711.
(45) Safarpour, M.; Vatanpour, V.; Khataee, A.; Zarrabi, H.; Gholami, P.; Yekavalangi, M. E. High Flux and Fouling Resistant Reverse Osmosis Membrane Modified with Plasma Treated Natural Zeolite. *Desalination* **2017**, *411*, 89−100.
(46) Yang, H.-C.; Xie, Y.; Chan, H.; Narayanan, B.; Chen, L.; Waldman, R. Z.; Sankaranarayanan, S. K. R. S.; Elam, J. W.; Darling, S. B. Crude-Oil-Repellent Membranes by Atomic Layer Deposition: Oxide Interface Engineering. *ACS Nano* **2018**, *12*, 8678−8685.
(47) Ghostine, R. A.; Shamoun, R. F.; Schlenoff, J. B. Doping and Diffusion in an Extruded Saloplastic Polyelectrolyte Complex. *Macromolecules* **2013**, *46*, 4089−4094.
(48) Garcia-Ivars, J.; Iborra-Clar, M.-I.; Alcaina-Miranda, M.-I.; Van der Bruggen, B. Comparison between Hydrophilic and Hydrophobic Metal Nanoparticles on the Phase Separation Phenomena during Formation of Asymmetric Polyethersulphone Membranes. *J. Membr. Sci.* **2015**, *493*, 709−722.
(49) Sadman, K. *Sadmankazi/QCM-D-Analysis-GUI v1.1*, 2018. DOI: 10.5281/zenodo.1482780.

DOI: 10.1021/acsami.9b02115
ACS Appl. Mater. Interfaces 2019, 11, 16018−16026